## 3.3 TABLE OF CONTENTS

## 3.4 ABSTRACT

A continuing experimental and theoretical investigation of Penning Fusion (PF) is described. In this approach, electrons are contained as a nonneutral plasma in a trap of the Penning type, *i.e.* one with both applied electrostatic (ES) and magnetostatic (MS) fields. This trap is configured with a small access through which electrons are injected and subsequently ejected and collected. Space charge of these contained electrons forms an electrostatic well for ion confinement. Technical limits on the space charge electric field limit average densities in such a system to less than $10^{18}$ $m^{-3}$. To achieve an interesting power density, particle density is enhanced by strong spherical focussing.

Progress on the previous PFX (Penning Fusion eXperiment) is reviewed, and all aspects of designing and constructing an advanced spherical trap are addressed. It is proposed to design, construct, and operate PFX-I (PFX-Ions), a 1.5 cm radius spherical trap with an advanced field configuration. A strong magnetic mirror provides part of the axial confinement of trap electrons, eliminating completely the need to apply high voltages to the front end of the machine. Operation up to 100 kV is possible. The electron cloud forms at nearly constant density within the front-end, producing a harmonic, electrostatic, spherical well for ion confinement. After diagnosing electron operation, ions will be introduced into PFX-I and large amplitude spherical oscillations will be stimulated. It is projected that up to several Watts of fusion power may be produced from deuterium operation, at a high fusion gain Q.

## 3.5.1 BACKGROUND AND SIGNIFICANCE

### Physics of PF (Penning Fusion)

This is a proposal to continue investigation[1-6] of a unique approach to fusion plasma confinement. In this approach, electrons are contained as a nonneutral plasma in a trap of the Penning type, *i.e.* one with both applied electrostatic (ES) and magnetostatic (MS) fields. This trap is configured with a small access through which electrons are injected and subsequently ejected and collected. Space charge of these contained electrons forms an electrostatic well for ion confinement. Technical limits on the space charge electric field limit average densities in such a system to less than $10^{18}$ $m^{-3}$. To achieve an interesting power density, particle density is enhanced by strong spherical focussing. For brevity, this approach will subsequently be referred to as the PF (Penning Fusion) approach.

Thus, two distinguishing physical features of our approach are: 1) Nonneutral electron plasma confinement; and 2) Spherical focussing. As developed subsequently in this proposal, unique technical challenges are associated with these features. Compared to toroidal confinement systems, a very different development path to a very different reactor product exists. While some details of our approach and its development may be regarded as speculative, progress to date has been excellent and there is no other known MFE approach which can lead to a similar reactor in which material wall problems are solved as effectively. These points are now developed in more detail. First, principles of the physics of electron and ion PF confinement are given.

Conceptually, one may consider the applied ES and MS fields of the trap to provide an effective, three-dimensional (3D) potential well for electrons. As shown in Fig. 1, these effective equipotentials form nested closed surfaces near

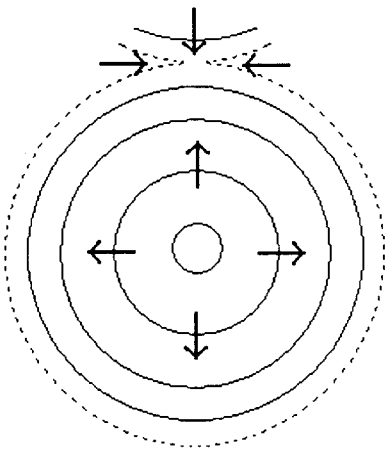

Figure1: Effective equipotentials for electrons in a PF trap. Arrows show the direction of increasing effective potential. The broken curve is the effective equipotential corresponding to the injection energy.

the bottom of the well. Near the top of the well (defined by the energy of injected electrons), the equipotentials form a divertor (or several divertors) at an energy slightly below the injection energy. Low-energy electrons are injected across the saddle at the divertor X-point and, in the absence of collisions, are collected at low energy after they pass out of the trap again over the saddle.

Since electrons are collected at an energy which is a fraction of the total well depth, electron energy confinement time $\tau_{Ee}$ is long compared to electron particle confinement time $\tau_e$. Thus, $\tau_e$, which is determined by the injection geometry, may be short compared to a typical Coulomb scattering time $\tau_{Ce}$, while $\tau_{Ee}$ may be greater than the required multiple of Lawson to achieve fusion energy gain. As detailed subsequently, it has been demonstrated, both by observation and by Fokker-Planck calculations, that under appropriate conditions it is possible to maintain a nearly monoenergetic electron distribution even in the presence of collisions. Electrons which downscatter in energy and become absolutely confined upscatter again against the higher energy injected electrons, leading to a steady distribution close to the ideal monoenergetic one.

To understand PF confinement, it is first necessary to consider how the electron well is produced by a combination of ES and MS fields. While it is possible to consider this in a 3D setting, only the case of rotational axisymmetry (2D) is necessary for PF and is the only case considered here. Suppose that an applied MS field with associated vector potential having only a component $A_\phi$ in the ignorable direction is combined with an applied ES field with applied electric potential $\Phi a$. It may be assumed that the electrons will form a rigid-rotor (RR) distribution, $fe = f(H - \Omega P_\phi)$, with $P_\phi$ the canonical angular momentum and H the total energy (both in the laboratory frame). Such a RR equilibrium is observed to rapidly form in a confined electron plasma and techniques for producing

such an equilibrium in a controlled manner are discussed subsequently. The argument

$$\overline{H} = H - \Omega P_\phi \ .$$

which may be considered the energy in the rotating frame, may be written as

$$\overline{H} = \frac{m_e}{2}\left(v_R^2 + v_Z^2 + \overline{v}_\phi^2\right) - e\left(\Phi + \Phi_A\right) \ , \qquad (1)$$

where $m_e$ is the electron mass and the relative velocity in the $\phi$ direction is given by conservation of angular momentum

$$\overline{v}_\phi = \frac{P_\phi + e\Psi}{2\, m_e R} - \Omega R \ ,$$

with $\Psi = R\, A_\phi$ is the magnetic flux and R the cylindrical radius. The magnetic effective potential is given by

$$\Phi_A = -\Omega\Psi + \frac{m_e \Omega^2 R^2}{2e} \ . \qquad (2)$$

This additional magnetic potential allows absolute electron confinement in a PF system.

PF ion confinement may now be considered. In PF designs, the two terms $\Phi$, and $\Phi_A$ will be comparable in magnitude. The effect of $\Phi_A$ on ion motion is reduced from that given in (2) for electrons by the mass ratio $m_e/m_i$, with $m_i$ the ion mass. Thus, $\Phi_A$ has negligible effects on ion confinement and only $\Phi = \Phi_a + \Phi_{sc}$, with $\Phi_{sc}$ the ES potential due to space charge, is effective in ion confinement. That is, ions are electrostatically confined in a PF system.

Several consequences of these PF features are: 1) Electron gyro orbit size is comparable to system size; 2) Ions are unmagnetized: 3) Large ES potentials exist (of order 100kV) in a system with particles of fusion relevant energies; 4) Absolute ion confinement requires that the electrons be nonthermal (so that they charge $\Phi_{sc}$ negative at the trap center).

## Technical Features of PF

At this point several dominant technical features of PF may be discussed. First, PF systems will be of one of two distinct types. Either they will consist of a large, quasineutral plasma surrounded by a very thin electron edge plasma or they will be of very small unit size. The former approach is being investigated in ongoing work elsewhere[7] and shares many features with conventional MFE systems.

The latter approach is considered here. In this case, the entire plasma is dominantly electrons whose unneutralized space charge determines the system size. For a spherical electron plasma of density $n_e$, the space charge potential is

$$\Phi_{SC} = \frac{e\, n_e\, \rho^2}{6\, \varepsilon_o} \ , \qquad (3)$$

where $\rho$ is the spherical radius and $\varepsilon_o$ the permitivity of free space. From (3) it follows that a potential of 301 kV will appear in a 1 cm radius system of density $n_e = 10^{18}$ m$^{-3}$. Practical considerations of minimum size, maximum density, and fusion relevant energies then dictate that system radius $a \approx 1$ cm, applied voltage $Vo \approx 100$ kV, and average density $ne \approx 10^{18}$ m$^{-3}$. Because 300 kV/cm cannot be supported against surface flashover, unique designs are required to avoid electrical breakdown in PF systems.

A second PF feature is the moderate mean density. To achieve a useful fusion power density, strong spherical focussing is used to enhance reactivity. This focussing may occur either by convergence of a radial ion beam distribution in a steady plasma (so called Spherically Convergent Ion Flow or SCIF approach) or by large amplitude ion oscillations in an oscillating plasma (so called Periodically Oscillating Plasma System or POPS approach). In the former case, volume (time) averaged reactivity increases linearly with convergence $a/r_c$, with $r_c$ the radius of the focus. In the latter case, reactivity increases as $(a/r_c)^2$. To achieve an average fusion power of 1 - 10 MW/m$^3$ a convergence of order 1000:1 is necessary. This requires that the intrinsic field errors (asphericity) be made extremely small. Combined with the already small size, tight component tolerances are required to achieve the desired convergence.

A third PF feature is the very small unit power output (3-300 W/sphere). It is proposed to use a massively modular approach to a final reactor product. Thus a 1GW electric plant might consist of $10^7$ 300W spheres. To achieve an acceptable fusion power core capital cost, a capital cost of less than a few dollars per sphere would be required. It is argued subsequently that such a low cost is achievable. Further the massive modularity allows two advantages otherwise unknown for MFE reactor concepts: 1) Modular maintenance at a "fuel rod bundle" level; and 2) Extremely low wall loading (of order $10^4$ - $10^5$ W/m$^2$)

Before describing the technical details of the proposed work, progress to date is reviewed.

## 3.5.2 PRELIMINARY STUDIES

The work proposed in the following section is based on preliminary experimental and theoretical work which provide preliminary confirmation of the principles of PF. Confinement and focussing of a nonneutral electron plasma has been demonstrated experimentally and confirmed by supporting theory. Additional theoretical calculations show that the proposed PFX-I will achieve strong ion focussing and associated high fusion reactivity. These preliminary studies are reviewed here.

### PFX Physics

The previously funded machine, the Penning Fusion eXperiment (PFX), achieves spherical convergence by means of an electrostatic, quadrupole field and a uniform, magnetic field. The electrostatic field is provided by an anode ring and two endcap cathodes shown in Fig. 2. When the proper relation is maintained between the magnitude of the magnetic and electric fields, a spherical well results for particles of a single charge-to-mass ratio. Near zero angular momentum trajectories originating at the center are reflected back on themselves by the well thereby forming a density focus at the trap center. This situation is depicted figuratively in Fig. 2.

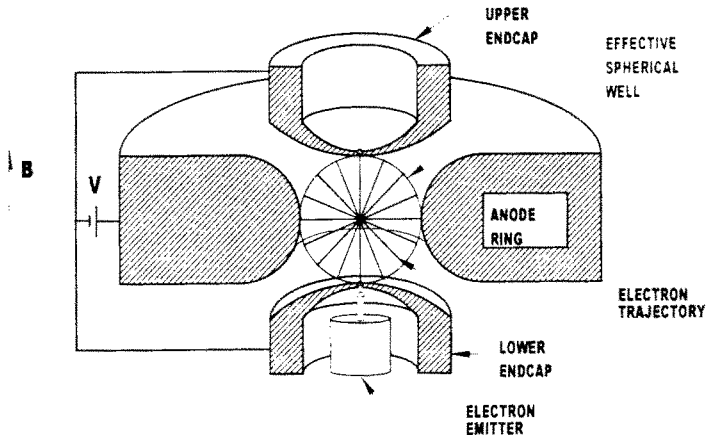


Figure 2: The PFX trap and electron emitter crystal. Also shown is a schematic representation of the spherical well and focused electron orbits.

PFX was designed to study electron focusing with anode voltages up to 10 kV. Electrons are loaded into the trap with low energy and angular momentum from a crystal electron emitter through a small hole in one of the endcap cathodes. Diagnostic information consists of electron scattering to the anode electrode or to a microchannel plate located outside of the trap. Access to this latter diagnostic is through a small hole in the endcap cathode opposite the electron emitter. A more complete description of the apparatus can be found in reference 4.

PFX has produced encouraging results. Figure 3 shows a sharp resonance in the electron current flowing to the anode as a function of anode voltage for a fixed magnetic field. The value of the anode voltage for which the peak occurs is exactly that for which the effective well is spherical. A complete discussion of this and other data confirming the existence of a spherical focus is beyond the scope of this document and can be found in references 5 and 6.

Peak densities at the center of the electron focus inferred from the experiment data and trap parameters exceed the Brillouin limit by as much as a factor of 35. Figure 4 shows the results of a numerical calculation using a bounce-averaged Fokker-Planck code applied to PFX conditions. The peak density is seen to be roughly 35 times the limiting Brillouin value, and the radius of the dense core is approximately 3 microns or 1% of the trap dimension. A more detailed discussion of this model can be found in reference 6.

The present PFX machine is inappropriate for the study of ion physics in a fusion-relevant regime. First, the vacuum fields in PFX provide focusing only for a single charge-to-mass ratio making it impossible to confine simultaneously dense deuterium and tritium plasmas. Second, the closed geometry of the system as presently implemented gives very limited diagnostic access to the trap volume and makes the application of high voltages (>40 kV) very difficult. Finally, the hyperbolic geometry provides for somewhat inefficient use of the trapping voltage with the actual well depth approximately 67% of the applied voltage. These limitations are removed in the proposed PFX-I design by forming a uniform density electron cloud and using its space charge field to confine and focus ions.

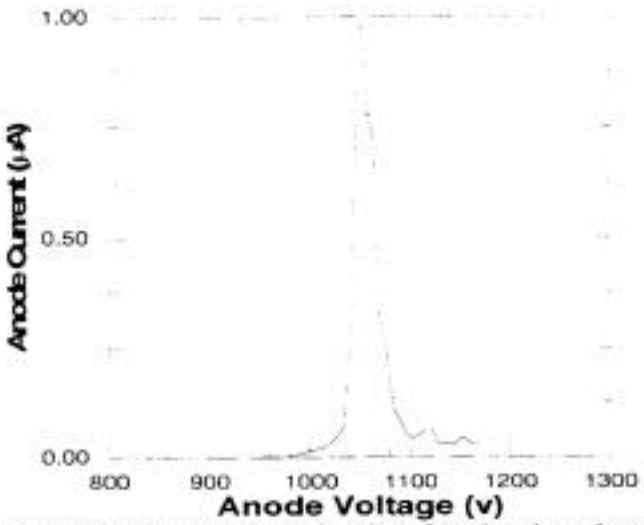


Figure 3: Electron current flowing to the anode electrode as a function of anode voltage for a fixed magnetic field. The sharp resonance is caused by strong scattering which occurs only when the effective well is spherical, indicating spherical focusing.

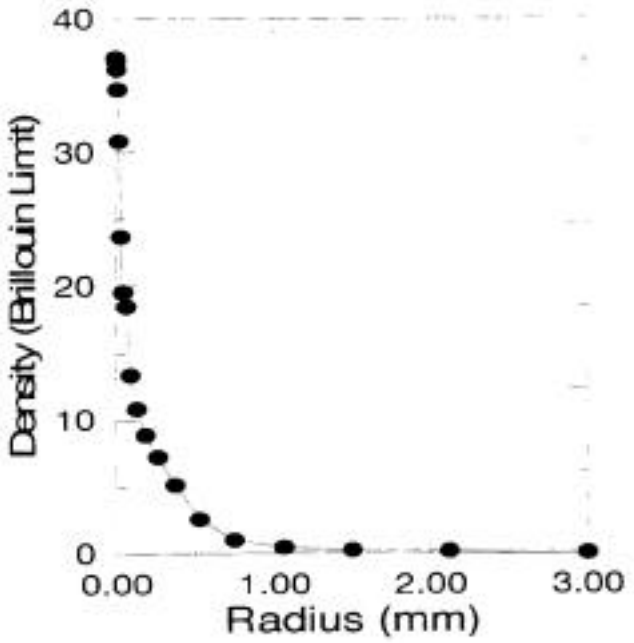


Figure 4: Calculated electron density profile. This distribution results when PFX parameters are used as input to a bounce-averaged Fokker-Planck code developed as part of this work.

## Electron Confinement for PFX-I

In order to eliminate the limitations associated with electrical breakdown among electrodes placed close to the PF plasma, the concept of PFX-I has been developed. In this proposed approach, an equipotential conductor surrounds the electron cloud. Thus, there are no electrical gaps across which breakdown may occur. Furthermore, this surrounding conductor acts as an anode, since the enclosed space charge causes the surface normal electric field to point away from the conductor. This means that the normal electric field may be raised to a high value, several times 100 kV/cm. In this way, large electron densities may be contained.

To prevent electrons from reaching the anode, a shaped magnetic field is applied so that monoenergetic electrons (at the injection energy plus a bit of "headroom") are not able to reach the anode conductor. If the conductor is shaped to form a sphere, interrupted at the two polar regions (an "onion" shape), a spheroidal electron cloud may be contained. In this case, the magnetic field, in the form of a strong magnetic mirror provides both radial and axial confinement, except in the polar regions, where the cloud is diverted.

## The Idealized Electron System

In order to more quantitatively introduce the PFX-I equilibrium configuration, it is useful to consider an idealized version. In this case, it is assumed that the external magnetic field may be shaped as desired. As discussed subsequently, practical considerations limit the achievable magnetic configurations, so a more ambitious design calculation is required for a realizable system.

For purposes of the ideal system, a well-posed problem is constructed by first giving the shape of a single onion conductor, which is assumed to be at ES ground potential. This conductor surface (CS) is also assumed to form a magnetic equipotential also, with effective voltage -Vo. From (2), this requires the magnetic flux on CS have the value

$$\Psi = \frac{V_o}{\Omega} + \frac{m_e \Omega R^2}{2e} \quad ,$$

Where $V_o$ Is the effective magnetic voltage, and $\Omega$ the constant rotation frequency.

The magnetic field everywhere in space is determined by finding the unique solution which produces the given flux on CS and which produces a uniform axial field at infinity whose magnitude matches
the flux density through the polar hole. That is

$$\Psi \approx \left( \frac{V_o}{\Omega R_m^2} + \frac{m_e \Omega}{2e} \right) R^2 \quad ,$$

at large distances from the system, where $R_m$ is the minimum radius along CS.

Finally, the electron density is found consistent with a given RR distribution. For the present purposes, it is sufficient to assume that the distribution is monoenergetic in the rotating frame. That is, $f_e = \delta(H - \Omega P_\phi - H_o)$. This gives the electron density as a function of the effective potential $\Phi + \Phi_A$ as

$$n_e = n_o \sqrt{[H + e(\Phi + \Phi_A)]/H_o - 1} \quad .$$

Thus, the equilibrium density is the solution of the nonlinear elliptic problem

$$\nabla^2 \Phi = \frac{e n_e}{\varepsilon_o} (\Phi + \Phi_A) \quad , \qquad (4)$$

where $\Phi_A$ is given by (2) from the previous solution for $\Psi$.

Based on previous far-field potential solvers used at LANL, a solution of (4) is found by iteration. For this, the density profile of the previous iterate is used to compute $\Phi$ from (4). Then the density is updated using a Marder-Weitzner relaxation.

A three-parameter description of CS is chosen by specifying an elliptic cross section spheroid of rotation interrupted at the pole by a tangent fairing with circular cross section which is convex toward the plasma and which continues until the surface normal is in the radial direction. Symmetry about the midplane is assumed throughout. Thus, with the midplane radius of CS normalized to unity, the three parameters are the axial length of the ellipse, the radius of the fairing, and the minimum radius of the fairing (where CS conforms to a uniform cylinder). This geometry is shown in Fig. 5. Note the orientation of the axes in Figs. 5-8.

Fig. 6 shows the effective vacuum magnetic potentials for the case of $b = 1$, $r_f = 0.1$, $r_m = 0.2$. Notice that the equipotentials conform to the sphere near CS, but become cylindrical near the system axis. If cold electrons are placed in such a potential, the space charge potentials will be the same as (the negative) magnetic potentials of Fig. 6. Such a configuration is clearly inappropriate for focussing ions.

Fortunately, when warm (monoenergetic) electrons are placed in the trap, the space charge potential becomes nearly spherical. If a very small electron density is added to this configuration, the electron density contours conform to this applied potential , according to $n_e(\Phi_A)$, with $\Phi$ negligible. In spite of this nonspherical density the space charge potential shows spheroidal contours (Fig. 7).

When the electron density is raised to higher values, the density deviates markedly from the applied potential, and the electrostatic space charge well deepens. Figure 8 shows the space charge for a somewhat optimized case. While the density may be raised yet more, this case achieves an electrostatic well depth of more than 41 % of the applied potential (over 40 kV for 100 kV applied). The conductor cross section has been made oblate to make the inner equipotentials more spherical.

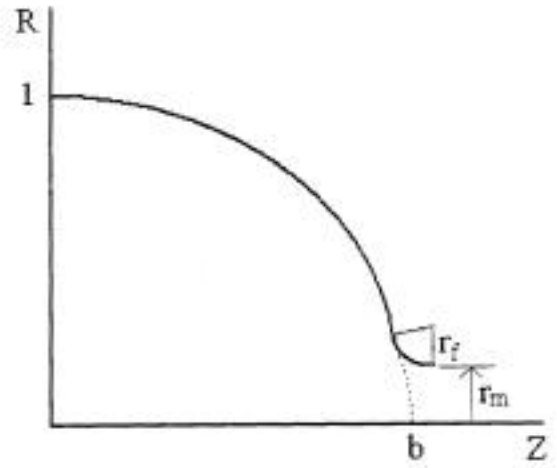


Figure 5: Geometric parameters for describing the conducting surface (CS) which forms the ideal PFX-I confinement volume. Symmetry about the Z=0 midplane is assumed.

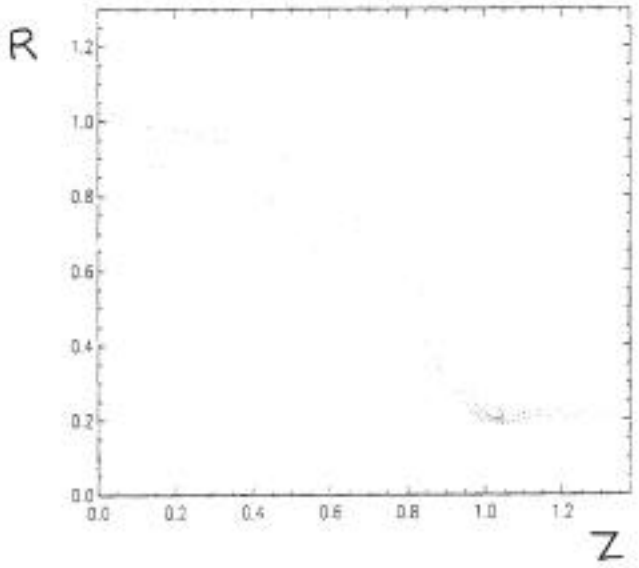


Figure 6: Magnetic effective equipotentials for circular boundary case. Conductor is shown in red.

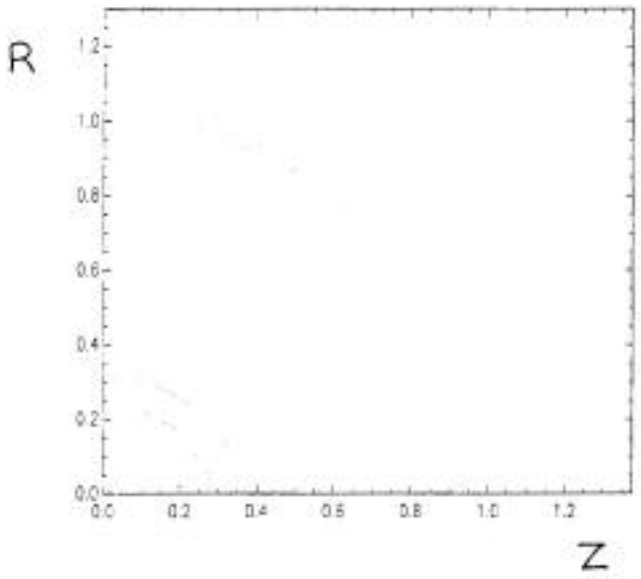


Figure 7: Space charge for low density case. Contours are uniformly spaced for harmonic well.

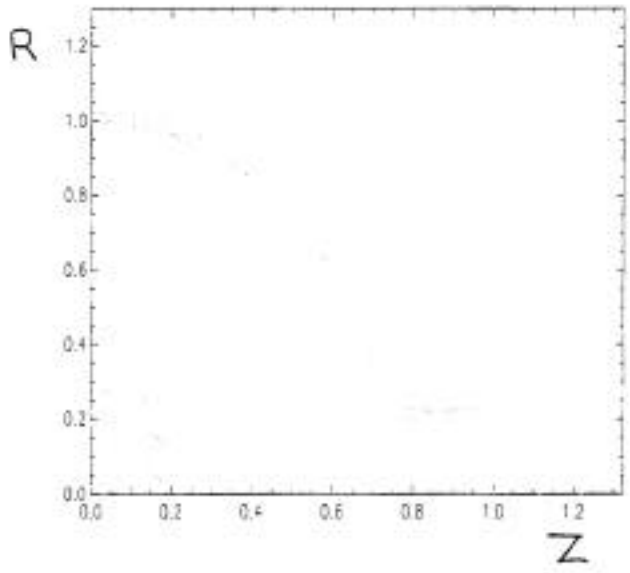


Figure 8: Space charge for high density case. Contours are uniformly spaced for harmonic well. Conductor has been made oblate and a cylindrical sleeve added to improve sphericity of interior equipotentials.

## Convergent Ion Physics

The electrostatic well produced by PFX-I electrons will be used to confine spherically convergent ions. Roughly speaking, the average ion density is maintained at a fraction of the average electron density, so there is a well which attracts ions toward the spherical center. Low energy ions placed in such a well will "fall" toward the center and form a focus there.

For some time, such research has followed the SCIF approach,[8] in which ions are maintained as a spherically convergent radial beam, producing high reactivity near the spherical center. While SCIF operation is certainly possible in PFX-I, several drawbacks appear:

1. A source of low-energy ions must be provided and any associated gas load must be isolated from the low-pressure required in the "front-end".
2. Fusion gain Q is limited by ion-ion collisions unless a central electrostatic well be formed for confinement of a thermonuclear ion component.[9]

These difficulties are avoided by the recently theoretically discovered POPS concept.[10] In this approach, cold ions undergo very large amplitude spherical radial oscillations which periodically produce a dense central focus with high fusion reactivity. Appendix C contains a draft preprint of a paper which is being prepared for submission. This paper describes the theory of POPS and shows that significant fusion reactivity may be expected for PFX-I parameters. Briefly, POPS operation involves the parametric driving of radial ion oscillations. This drive may be provided by low amplitude oscillation of the electron density, for example by modulation of the electron source. It is found that these oscillations will grow to a large amplitude, assuming the ion space charge is neutralized during the high-compression phase of the cycle by trapping of low temperature electrons. The ion density at the collapse is limited only by the particular adiabat on which the ions may be maintained. For an ideal spherical, harmonic well and a Gaussian ion density profile, there is no effect of ion collisions, since the distribution is everywhere an exact Maxwellian. A large transparency of the configuration to neutrals assures that the ions will remain on a room-temperature adiabat, implying extreme limiting convergence, several 1000:1 in radius. Fusion rates for PFX-I are in the several Watt range, implying a power density of order 1 $W/cm^3$ and a high Q.

## 3.5.3 RESEARCH DESIGN AND METHODS

### Overview

The technical work proposed here will provide a complete proof-of-principle of the PF concept. The focus of this work is producing a deep (up to 100 kV) electrostatic well for ion confinement and studying spherically convergent ion physics in such a system. Specifically, we propose to:

1) Design and construct a PF trap to produce a uniform density electron "sphere" with excellent electron energy confinement.
2) Operate this trap with electrons over a range of applied voltage, magnetic field, and electron density and diagnose the results.
3) Introduce ions via a static deuterium gas fill and study how to produce large spherical convergence by the Periodic Oscillating Plasma Sphere (POPS) approach.
4) Optionally, introduce low-energy ions from an external ion source and study spherical convergence by Spherically Convergent Ion Flow (SCIF).

### Practical Constraints and the Design Problem

PFX-I represents an ambitious physics step for the development of the PF concept. There are two major phases of this development. First, the desired electron sphere must be realized, and its properties diagnosed. Second, ions must be introduced into the system and their oscillating behavior diagnosed. In order to even realize the desired electron configuration, several engineering and physics goals must be accomplished:

1. The desired magnetic configuration must be approximated within CS.
2. The ES configuration must be adapted to an achieved magnetic configuration.
3. The desired RR monoenergetic electron distribution must be formed and maintained.
4. Electron density modulation at the desired level and frequency must be accomplished.
5. Ions must be provided at a controlled rate to the electron cloud.

In this section, strategies for addressing each of these goals are described. In cases where significant technical risk is identified, an early prototype experiment is outlined, and possible backup strategies enumerated. The magnetic design is first considered. Because of the small size of the CS, it is not possible to use external coils to produce the desired magnetic field. The only applicable technologies appear to be shaping of an externally applied magnetic field by iron components, and/or permanent magnets. It is proposed to use a combination of these two technologies to produce the best approximation to the ideal MS field of the previous section ("The Idealized Electron System"). The boundary condition desired on CS is that the magnetic flux should be that of a uniform moderate (1.4 kGauss for a 1.5 cm radius PFX-I) field plus a constant offset, representing a high flux density (corresponding to 1.85 T for PFX-I) near the polar regions. A conceptual PFX-I "front end" is shown in Fig. 9.

In this concept, an externally applied uniform magnetic field is produced by a superconducting solenoid. This uniform field is largely shielded from the front-end region. The magnetic shield consists of high-$\mu$ iron and is interrupted at the polar regions by two holes which form the electron injection/ejection divetor regions. The flux passing through these holes provides the polar offset constant flux. The uniform-field part of the flux is produced by arranging for flux leakage at a controlled and constant rate through the shield. For this purpose, the shield if formed as a laminate, with alternating thin layers of nonmagnetic material. This produces an effective magnetic resistivity which is inversely proportional to the radial area of the shell. By tailoring the cross section as indicated in Fig. 9, the leakage flux rate may be controlled to the proper value. An equatorial gap is provided for vacuum pumping and diagnostic access. Additional small holes may be placed drilled through the shield to provide additional access chords.

For small enough applied fields, such a shield will produce a flux close to the desired ideal constant-field plus offset along the inner surface. In practice, it is desired to raise the field to the highest value consistent with saturation of the iron shield. In order to evaluate this concept close to this saturation limit, a prototype experiment is planned. In this prototype, a prototype shield will be placed into a warm-bore superconducting solenoid magnet and the resulting magnetic field measured directly with a high-resolution Hall probe. Such measurements may be done without vacuum, so accessibility is optimal. As described in the proposed schedule, we will employ an experimental graduate student this summer to acquire these data.

Once the MS configuration is carefully measured, the ES field may be compensated to optimize the spherical well. For this, the design code used to generate the examples of the previous section will be adapted to input the measured MS field. The shape of CS will then be determined to optimize the well. Finally, the desired shape may be machined into the inner surface of the shield. For this purpose, an insert of nonmagnetic material is placed inside the shield, and its inner surface is carefully machined.

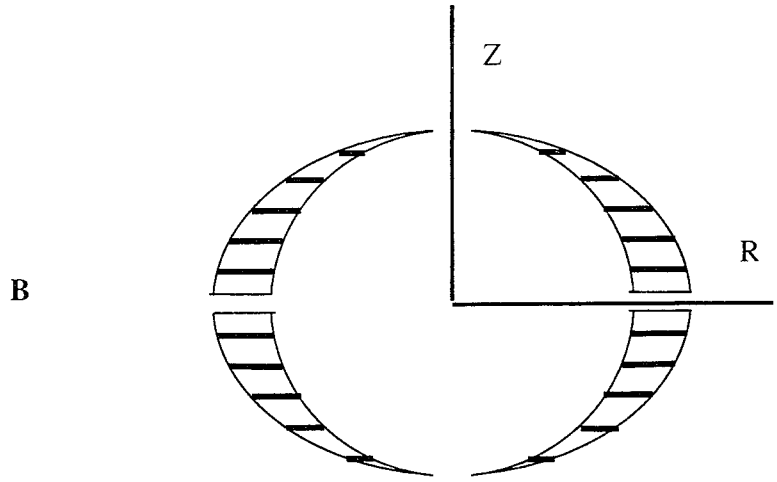


Figure 9: Magnetic concept for PFX-I front end.

Because the RR distribution is observed to be a metaequilibrium for nonneutral electron plasmas, the desired distribution may be formed by injection of electrons with a given mean energy <H> and a given mean angular momentum $<P_\phi>$. If the confinement time of the electrons is longer than the time to reach rigid rotation, a RR distribution will be formed. This time is observed to be a few 100 to 1000 rotation periods,[11] which is between $10^{-8}$ and $10^{-7}$ s. Thus, if $\tau_e$ is greater than this relaxation time, a RR distribution will be formed. A conservation law based theory of this process is described in Appendix D. In PFX-I, an electron source of the type shown in Figure 10 will be used. This source uses a radially-extended cathode. In combination with a magnetic shield (a simple iron sleeve placed in the source region, the amount of magnetic flux intersecting the cathode is controlled, fixing $<P_\phi>$ at the source. Since <H> = H is fixed at the constant cathode potential, the control of the cathode magnetic flux will set the rigid rotation rate of the electron configuration.

As discussed in the subsequent paragraph, it is critical that $\tau_e$ be sufficiently small, in order that modulation of the electron density be accomplished on the required ion oscillation time scale. Thus, it is a high priority to demonstrate formation of the required RR distribution and to observe the time scale for relaxation to such a state. A prototype experimental test of formation of a RR cloud is planned using an available cylindrical trap. This trap operates at low potentials and low densities, so the required electron source is quite modest. A simple Tungsten wire loop placed in the uniform field will produce the required $<P_\phi>$.

Electron density modulation is required for POPS operation. This will be accomplished in PFX-I by including a control grid in the electron source (Fig. 10). The grid voltage determines the electron current injected from the cathode, as a function of time. Since the injection current is not too large, it is practical to achieve 100 % modulation of this current, at the source. The resulting density modulation will depend on the modulation frequency and $\tau_e$. The relative modulation is easily seen to be $f = 1/[1+(\omega \tau_e)^2]^{1/2}$, where $\omega$ is the required oscillation frequency, $\omega = 6 \times 10^8\ s^{-1}$ (Appendix C). For a density modulation of $f = 10^{-3}$ it is then required that $\tau_e$ be less than 1.7 μs. Since the total inventory in PFX-I will be about $N_e = 2 \times 10^{12}$ electrons, the source current must be greater than about 200 mA. Such a current is achievable with a heated cathode, and it may even be possible to operate with a cold cathode, depending on neutral pressure.

As shown in Fig. 10, electrons emitted from the cathode and reflexed back there from the front-end will be collected at a fractional rate by a collector located behind the cathode. A small hole in the center of the cathode will allow this collection at a controlled rate. For PFX-I parameters estimated above, this fraction is about $10^{-3}$. In ideal operation, no electrons pass to the anode potential, and all return and are collected behind the cathode. Thus, the major power input is through the low-voltage collector circuit.

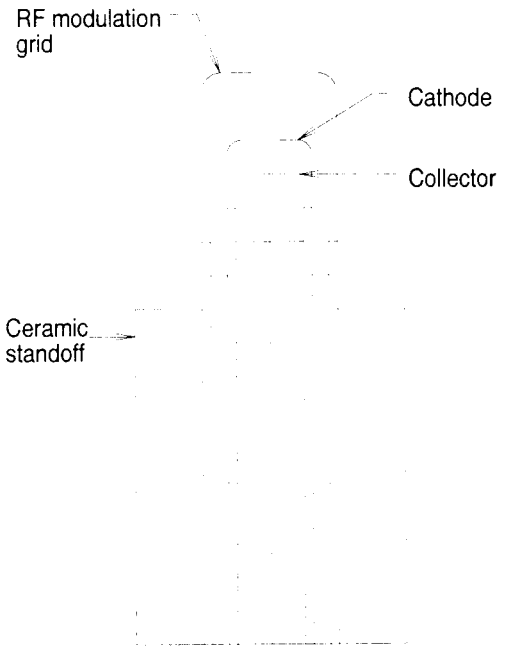


Figure 10: Sketch of electron source. Triaxial conductors are all held at nominal high voltage.

To provide ions to PFX-I, a static neutral deuterium fill will be used. The required neutral pressure is quite low, since the ion inventory is determined by a balance between the ionization rate due to energetic electron impact, and the loss rate from the deep electrostatic well. It appears that ion confinement is near absolute for POPS operation, since the average ion thermal energy is so small. Ions are pumped from the well by overdriving the radial oscillations. This requires a power supplied through the electron channel which raises ions from their source energy to the top of the well. For a 100 kV well in a 1.5 cm radius sphere, this power is calculated from the electron-impact ionization cross-section and the electron inventory, using the fact that a uniform source requires 40 % of the well depth to raise an average ion to the top of the well. The required electron power is $3.6 \times 10^6$ W/Torr $P_o$, where $P_o$ is the neutral pressure. Since the electron power in PFX-I is a few Watts, $P_o$ should be in the range of a few x $10^{-7}$ Torr. Thus, PFX-I will be designed for excellent base pressure and with careful gas control.

## Experimental Arrangement and Diagnostics

The overall experimental arrangement of PFX-I is shown in Fig. 11. The electron source of Fig. 10 extends through a vacuum flange at the top of the trap volume. Emitted electrons are guided magnetically to the front-end onion, fill the front-end volume and pass through a symmetric hole in the bottom of the front end. From there, they are again magnetically guided to a reflector, which is a floating electrode held from ground by a high dielectric strength ceramic post. The electron source and its associated low-voltage electronics are raised to a high negative potential ( up to 100 kV) by an external power supply. Figure 12 shows the proposed HV layout which is discussed subsequently. The only other high-voltage component in the trap is the electron reflector, which floats to a potential close to the cathode. The only breakdown paths which must be protected are along the dielectrics at the source and reflector. These will be of high-purity Alumina with carefully prepared surfaces to avoid flashover. All remaining components of the trap will be at or near ground potential.

The Penning electron gun power source consists of a floating "hot deck" (Fig. 12) cylindrical chassis with a 3" diameter to fit within the solenoidal bore of the super-conducting magnet. The chassis mounts to a vacuum flange with a high voltage multi-conductor ceramic vacuum feed-through. To maintain proper high voltage integrity, the space between the vacuum flange and hot deck chassis is potted. The electron gun is mounted directly to the feed-through post with a re-entrant dielectric barrier to improve vacuum hold-off characteristics. Within the hot deck, various power supplies and a RF driver may be located to power and control the electron gun source. Fiber optic control and monitor systems will be utilized to ensure proper operation of the gun power systems. The electron beam voltage is provided by an external power supply. Power for the hot deck is provided by a low capacitance high-voltage isolation transformer. The completed assembly requires a dielectric wrap to prevent breakdown between the hot deck and the solenoid bore. The control hardware and power supply are contained in an interlocked control rack, with PVC piping providing a protective conduit for control and HV cabling between the rack and hot-deck chassis. Most hardware is available except for the specialized construction requirements necessary to meet the system physical constraints. A custom high-voltage vacuum feed-through is required in addition to the cylindrical hot-deck chassis. The estimated cost break-down is included in Sec. 3.7.

We will probe the electron density in the system spectroscopically. The system is designed to provide a background vacuum on the order of $10^{-9}$ Torr and will have the capability of introducing a static fill of a variety of gases. Static fill pressures from $10^{-8}$ to $10^{-4}$ Torr should be easily attainable through a Granville-Phillips leak valve attached directly below the trap. The vacuum wall in the midplane of the system will be 7052 glass which has a transmission window from 400 nm to 2000 nm allowing external counting of photons from many atomic transitions including the hydrogen Balmer-$\alpha$ line (656.28 nm) or the 587.5 nm transition in helium. A standard photomultiplier tube and signal processing electronics can be used for data acquisition. Photons from other unwanted

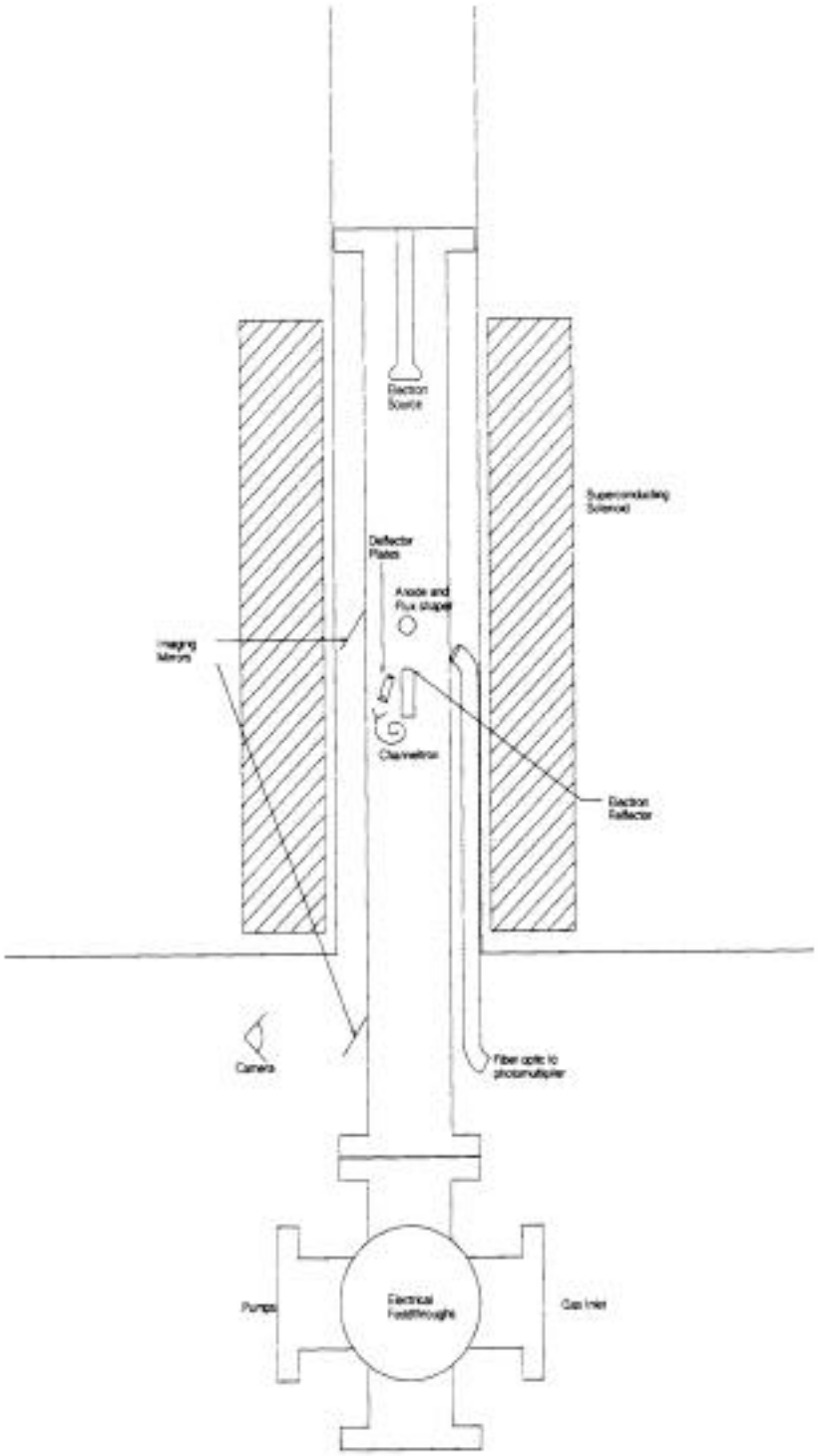


Figure 11: PFX-I trap experimental arrangement and diagnostics layout.

transitions which are not attenuated by the vacuum wall can be eliminated by means of narrow band filters on the input to the photomultiplier tube.

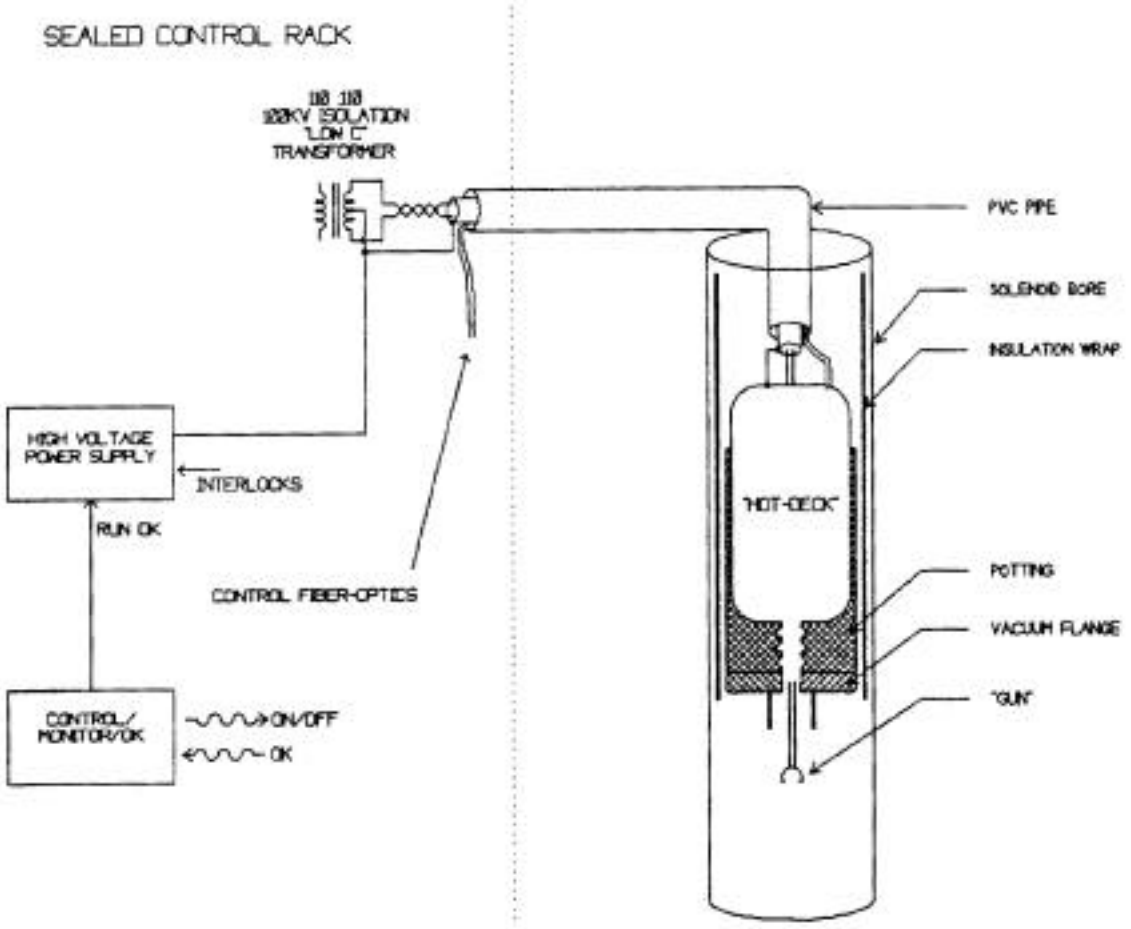


Figure 12: PFX-I high-voltage system layout.

Initial operation will be limited to hydrogen or helium gas fill. At the high energies of interest here (10 keV - 100 keV), the binding energy of molecular hydrogen becomes negligible, and we can treat the molecule as simply two hydrogen atoms. This is born out by the convergence of the $H_2$ ionization cross section to twice that for atomic hydrogen at 10 keV impact energy.[12] The relevant processes for hydrogen, then, are

(1) $H(1s) + e^- \rightarrow H(3p) + e^-$
(2) $H(3p) \rightarrow H(2s) + h\nu$

The transition probability for the 3p to 2s decay is well known, and the excitation cross section can be calculated for energies in the 10-100 keV range of interest here using the Bethe-Born formalism.[13]

The rate at which photons are produced in the trap volume is $n_e n_n Q v A_{32}/A$. Here $n_e$ is the electron density, $n_n$ is the neutral density, Q is the excitation cross section , v is the electron velocity, $A_{32}$ is the transition probability for the Balmer-$\alpha$ line, and A is the total transition probability out of the 3p state. Assuming a hydrogen pressure of $10^{-5}$ Torr and a detector fractional solid angle of $6 \times 10^{-4}$ we get an expected signal ranging from $2 \times 10^9$ $s^{-1}$ to $7 \times 10^9$ $s^{-1}$ for 10 to 100 keV energy range for the maximum expected electron densities ($3 \times 10^{10}$ $cm^{-3}$ to $3 \times 10^{11}$ $cm^{-3}$). Obviously, lower electron densities will result in lower photon fluxes, but should still be well within the counting capabilities of a photomultiplier tube.

Helium can also be used in the system. The 585.7 nm transition in neutral Helium can be used in exactly the same fashion as outlined above for the Balmer-α line. Here one avoids the complication presented by the molecular species but must take into consideration the $He^+$ spectrum. This is, of course, hydrogenic with wavelength essentially one-fourth the corresponding lines in neutral hydrogen. Hence, the majority of lines will be shifted out of the transmission window of the glass vacuum envelope. The nearest line which might interfere is the Paschen-α line ($\lambda \equiv 469$ nm in $He^+$), however this transition should account for at most a few percent of the photons emerging from the trap volume and can be attenuated by the use of filters.

Ion diagnostics will include measurement of the number and energy of protons emerging from the trap volume. After ionization and acceleration of neutral gas by the high energy electrons, some fraction of the protons will escape the trap. The number emerging from the well will depend on the density and energy of the trapped protons as well as the electron density and energy. The number can be counted with high sensitivity by a channel electron multiplier. Energy analysis can be accomplished by means of a set of parallel deflector plates. Two 1cm long plates separated by 0.5 cm with a 5 kV potential difference between them will deflect a 100 keV proton by approximately 3 degrees. Entrance and exit apertures will reduce spurious counts from neutrals, photons, or other charged particles.

## Program Plan

The design and construction of PFX-I will proceed by first prototyping the most critical components of the machine. Two prototypes presently identified are magnetic probing of a prototype shield assembly for the front end, and RR prototype for studying how to control rotation rate in electron traps with a throughput of electrons. The major hardware for both of these prototypes exists. A warm bore superconducting magnet will provide the magnetization for the magnetic prototype. We will purchase a small Hall probe and borrow a mechanical positioner to speed data acquisition. Measurements will be accumulated summer 97 with the assistance of a GRA. A second GRA will set up and operate an existing cold bore electron trap. Electrons will be produced from a heated Tungsten ring emitter and rotation rate and density of the existing cloud will be observed by amplification of segmented electrode signals. This publishable data will test the theoretical projections of Appendix D.

A complete engineering design will be completed by the end of CY 97, at which time, a design review will be held. This process proved invaluable in the design and subsequent construction of PFX, and a similar panel of internal and external experts in various aspects of PFX-I design issues will meet for a one day review early in CY 98. Construction of PFX-I will follow during the first half of CY 98, with first electron plasma expected early in FY 99.

Operation of PFX-I and upgrades to the trap hardware will provide physics data during FY 99 and FY 00. The project will be completed by end of FY 00, with data on ion operation. During the entire course of the PFX-I project, there will continue to be a close integration of theory and experimental efforts. Costing for PFX-I included in this proposal package includes approximately 20 % for theoretical support, which will contribute directly to the design process, as well as to experimental data analysis.

## Long-term Development Path

As discussed previously, the development path for PF differs markedly from that for conventional MFE (that is, moderate density toroidal confinement) systems. While a complete development of this subject is beyond the scope of this proposal, and we have chosen to emphasize the physics and experimental technical details, a few comments are useful to motivate the place of PF in the OFES portfolio, and as a plasma technology with important applications to problems of National importance.

It is obvious that success with PFX-I would provide the technical basis for an extremely valuable source of MeV neutrons. With a few Watts of input power, and with engineering to provide hermetic sealing, permanent magnets, and ruggidization, a small, portable source of D-D neutrons in the range of $10^{13}$ $s^{-1}$ would be possible. Present sources used, for example, for petroleum reservoir logging have comparable sizes and power inputs and generate of order $10^8$ D-T neutrons/s. The usefulness of a 100,000 fold increase in neutron output is obvious.

Thus, on a time scale of five years or so, the research proposed here might offer a commercial spin-off of tremendous commercial value. One may further ask about the applicability of PFX-I to fusion electric generation or other large portable or fixed point power applications (such as space power). A novel feature of PF is the extremely small size. We imagine a reactor with advanced magnetic and electrostatic design. In the projected system, 300 kV electrons are contained in a 1 cm spherical radius system. This implies an electron density of $10^{18}$ $m^{-3}$. Assuming the mean ion density is equal to this, and that ions remain on a room temperature adiabat, the time-averaged power output from POPS operation would be 164 W with D-D operation. Based on classical electron collisions, the fusion Q would be greater than 500, so the electron channel will not directly limit Q. Q is set by ion losses due to fusion. For the assumed parameters, the ion loss power is 13 W. If this power were all required to be supplied from the electron source, Q = 12 results. However, since the escaping charged products are in a deep electrostatic well, there is actually a direct conversion of twice the ion loss power (thermal energy at burn is ½ well depth). Thus, 13 W of excess fusion power is actually coupled directly to the

electrons, through ion oscillations. Such a reactor is as good as an ignited one, since electrical power is actually extracted from the "heating" system.

A massively modular approach to organizing order $10^7$ such spheres results from the observation that the electrons exiting a first sphere adjacent to the electron source may be used to fill a second sphere located axially adjacent to the first. This allows packing spheres like a "string of pearls" into a long "fuel rod" like array. Since each sphere consists only of passive components, this

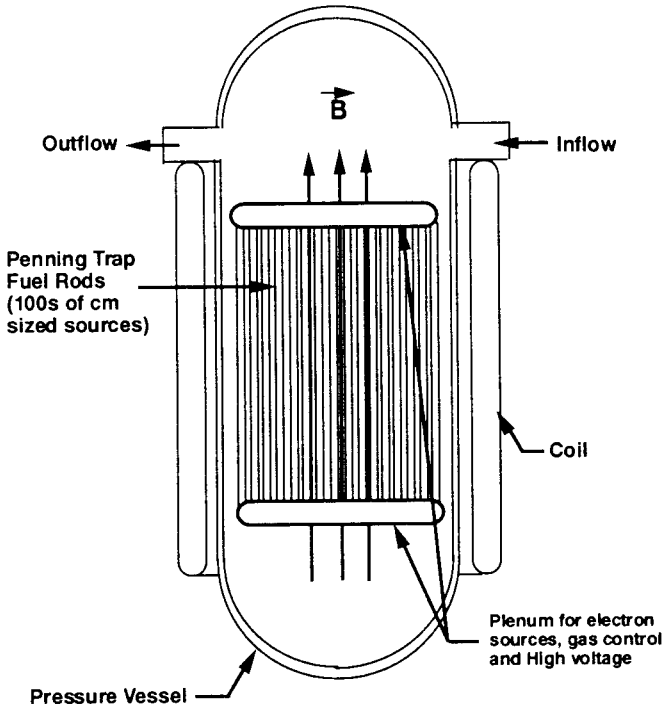


Figure 13: Sketch of principal components of PF based fusion reactor core.

arrangement requires no additional components. Only the magnetic design must be modified to produce the desired axially periodic array of spherical regions. Since the far magnetic field is uniform, a series of these rods may be located parallel to one another, as shown in Fig. 13, and may share a common heat exchanger, magnet, vacuum and gas system, and high-voltage system. We will not prove here that such an arrangement could lead to a cost-effective reactor, but only note that the neutron wall loading problem which has received recent attention[14] is solved in this approach. Further, the neutronics of such a reactor are vastly simplified, since no breeding is required, and no criticality need be maintained. The coolant water may be loaded with a high concentration of benign neutron absorbing material, such as boron. It should be noted that the neutron wall loading on a single cell PFX-I, upgraded to the desired reactor parameters of increased well depth is the same as that in the final reactor embodiment, so the appropriate engineering data base will exist if physics success is achieved!

## Milestones and Deliverables

- 10/97 Complete magnetic prototype
- 11/97 Optimum POPS operation calculated for PFX-I
- 12/97 Complete engineering design for PFX-I
- 1/98 Complete rigid-rotor control prototype
- 1/98 Design review held at LANL
- 5/98 All components procured
- 10/98 First electron operation of PFX-I
- 10/99 First ion operation of PFX-I

## 3.6 REFERENCES


[1] D. C. Barnes and L. Turner, *Phys. Fluids* **B4**, 3890 (1992).

[2] D. C. Barnes, L. Turner, and R. A. Nebel, *Phys. Fluids* **B5**, 3651 (1993).

[3] D. C. Barnes, L. Turner, R. A. Nebel, and T. N. Tiouririne, *Plasma Phys. and Control. Fusion* **35**, 929 (1993).

[4] M.M. Schauer, T.B. Mitchell, M.H. Holzscheiter, and D.C. Barnes. Submitted to *Rev. Sci. Inst* (1997).

[5] T.B. Mitchell, M.M. Schauer, and D.C. Barnes, *Phys. Rev. Lett.* **78**, 58 (1997).

[6] D.C. Barnes, T.B. Mitchell, and M.M. Schauer, to appear *Phys. Plasmas*, May 1997.

[7] R. W. Bussard, U.S. Patent #4,826,626 (1989); R. W. Bussard and N. A. Krall, *Fusion Technology* 25, 228 (1994); N. A. Krall *et al.*, *Phys. Plasmas* 2, 146 (1995).

[8] R. L. Hirsch, *J. App. Phys.* **38**, 4522 (1967); T. A. Thorsen, R. D. Durst, R. J. Fonck, and L. P. Wainwright, *Phys. Plasmas* **4**, 4 (1997); *see also Ref. 7*.

[9] W. M. Nevins, *Phys. Plasmas* **2**, 3804 (1995).

[10] R. A. Nebel, D. C. Barnes, in preparation; *see also Appendices C and E.*

[11] C. F. Driscoll and K. S.Fine, *Phys. Fluids* **B2**, 1359 (1990); T. B. Mitchell and C. F. Driscoll, *Phys. Fluids* **8**, 1828 (1996).

[12] C.F. Barnett, "Atomic Collision Properties" in *Physics Vade Mecum*, Herbert Anderson, Ed. Published by AIP Press.

[13] S. Trajmar, J.W. McConkey, and I. Kanik, "Electron-Atom and Electron-Molecule Collisions" in *Atomic, Molecular, and Optical Physics Handbook*, G.W.F. Drake, Ed. Published by AIP Press.

[14] W. E. Parkins, *et al.*, *Phys. Today*, p. 15, March 1997.